

Osteogenic Differentiation of Bone Marrow-Derived Mesenchymal Stem Cells in Electrospun Silica Nonwoven Fabrics

Kazutoshi Iijima,^{†,‡} Shohei Ishikawa,[‡] Kohei Sasaki,[§] Mineo Hashizume,[†] Masaaki Kawabe,[§] and Hidenori Otsuka^{*,‡,||}

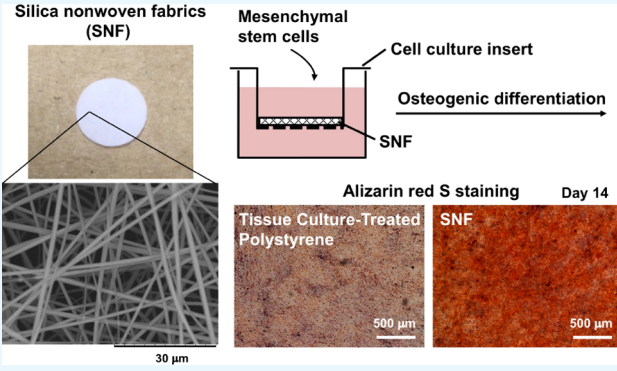
[†]Department of Industrial Chemistry, Faculty of Engineering, Tokyo University of Science, 12-1 Ichigayafunagawara-machi, Shinjuku-ku, Tokyo 162-0826, Japan

[‡]Graduate School of Science and ^{||}Department of Applied Chemistry, Faculty of Science, Tokyo University of Science, 1-3 Kagurazaka, Shinjuku-ku, Tokyo 162-8601, Japan

[§]Japan Vilene Company Ltd., 7 kita-Tone, Koga, Ibaraki 306-0213, Japan

Supporting Information

ABSTRACT: Silica nonwoven fabrics (SNFs) with enough mechanical strength are candidates as implantable scaffolds. Culture of cells therein is expected to affect the proliferation and differentiation of the cells through cell–cell and cell–SNF interactions. In this study, we examined three-dimensional (3D) SNFs as a scaffold of mesenchymal stem cells (MSCs) for bone tissue engineering applications. The interconnected highly porous microstructure of 3D SNFs is expected to allow omnidirectional cell–cell interactions, and the morphological similarity of a silica nanofiber to that of a fibrous extracellular matrix can contribute to the promotion of cell functions. 3D SNFs were prepared by the sol–gel process, and their mechanical properties were characterized by the compression test and rheological analysis. In the compression test, SNFs showed a compressive elastic modulus of over 1 MPa and a compressive strength of about 200 kPa. These values are higher than those of porous polystyrene disks used for in vitro 3D cell culture. In rheological analysis, the elastic modulus and fracture stress were 3.27 ± 0.54 kPa and 25.9 ± 8.3 Pa, respectively. Then, human bone marrow-derived MSCs were cultured on SNFs, and the effects on proliferation and osteogenic differentiation were evaluated. The MSCs seeded on SNF proliferated, and the thickness of the cell layer became over 80 μm after 14 days of culture. The osteogenic differentiation of MSCs on SNFs was induced by the culture in the commercial osteogenic differentiation medium. The alkaline phosphatase activity of MSCs on SNFs increased rapidly and remained high up to 14 days and was much higher than that on two-dimensional tissue culture-treated polystyrene. The high expression of *RUNX2* and intense staining by alizarin red s after differentiation supported that SNFs enhanced the osteogenic differentiation of MSCs. Furthermore, permeation analysis of SNFs using fluorescein isothiocyanate-dextran suggested a sufficient permeability of SNFs for oxygen, minerals, nutrients, and secretions, which is important for maintaining the cell viability and vitality. These results suggested that SNFs are promising scaffolds for the regeneration of bone defects using MSCs, originated from highly porous and elastic SNF characters.



INTRODUCTION

In tissue engineering for regenerative medicine and in vitro assay technology, a three-dimensional (3D) cell culture system mimicking in vivo environment provided higher cellular functionality than a traditional two-dimensional (2D) cell culture.¹ There are various culture methods of cells in a 3D system, for example, spheroid formation^{2,3} and seeding in scaffolds such as polymer hydrogels,⁴ porous materials,⁵ and fibrous fabrics.⁶

Recently, mesenchymal stem cells (MSCs) have been receiving much attention as a cell source for cell therapy and tissue engineering applications.⁷ The MSCs isolated from bone marrow⁸ and adipose tissue⁹ have the ability to differentiate

into various types of cells in mesodermal lineages, such as osteoblasts,¹⁰ chondrocytes,¹¹ adipocytes,¹² myocytes,¹³ and cardiomyocytes.¹⁴ Bone regeneration using MSCs is a new therapeutic approach for large bone defects.¹⁵ MSCs were transplanted with scaffolds and differentiated into osteoblasts and osteocytes, and secreted bone matrices were connected with the surrounding bone tissues.

For these cell differentiations, particularly MSCs, 3D fibrous fabrics prepared by electrospinning techniques showed highly

Received: May 25, 2018

Accepted: August 20, 2018

Published: August 30, 2018

suitable properties¹⁶ because of their morphological similarity to that of the fibrous extracellular matrix (ECM). Nonwoven nano- and microfibrillar scaffolds of polymers such as poly(ϵ -caprolactone),¹⁷ poly(ethylene terephthalate),¹⁸ poly-L-lactide,¹⁹ polyethersulfone,²⁰ and their compositions²¹ including other components have been developed. Fabrics prepared by electrospinning are not limited to polymers. The 3D silica nonwoven fabrics (SNFs) with interconnected highly porous microstructures have also been developed by electrospinning through the sol–gel process^{22–24} and are used for cell culture in a differentiated state.^{25,26} The silica obtained by the sol–gel process shows high biocompatibility and bioactivity.²⁷ Many interconnected pores were provided by the random orientation of the silica fibers, and cells can migrate and grow, preventing shrinkage because of their enough mechanical strength. SNFs have been applied for the construction of 3D tumor models²⁵ and a coculture system.²⁶ Cancer cells cultured in SNFs showed poorer response to anticancer agents by the upregulation of genes such as *BCL2*, and potentials of SNFs for the construction of 3D tumor models in vitro were suggested.²⁵ We have clearly demonstrated the utility for a tissue-engineered construct: a fibroblast migrated and penetrated in SNFs and showed remarkable growth rates compared to the traditional 2D culture.²⁶ Furthermore, the functions of hepatocytes cocultured with the fibroblast in SNFs were significantly higher than those cocultured with the 2D fibroblast because of the abundance of fibroblast-secreted soluble factors, which is important for maintaining the function of hepatocytes.²⁶

One of silica-based materials, bioactive glass containing additives such as sodium oxide, calcium, and phosphate, has been widely used as an implantable material for bone regeneration because of its osteoconductive, osteoprotective, and osteoinductive properties.^{28–31} For example, the osteoconductivity of polyethersulfone nanofibers was enhanced by loading with bioactive glass nanoparticles.²¹ Bioactive glasses derived by the sol–gel process exhibit high bioactivity and resorbability because of their macroporous and mesoporous structures.³² In addition to bioactivity and resorbability, the scaffolds for bone tissue regeneration need to act as a 3D container of cells in vitro and in vivo. The scaffolds consist of macroporous structures with an interconnected network, allowing cell migration, tissue ingrowth, and vascularization.³³ By utilizing the scaffolds promoting cell attachment, migration, and ideally inducing osteogenesis,³⁴ the engineered bone tissue ready for implantation can be constructed in vitro. This construct should have mechanical strength mimicking that of the inherent bone. Considering from our previous study,^{22–26} SNFs can be highly useful as osteoinductive and biomimetic materials with high moldability, working not only for the in vitro cell assay system but also for implantable cell scaffolds for bone defects.

Here, we examined 3D SNFs as a scaffold of MSCs for bone tissue generation. Culture of MSCs in SNFs is expected to affect their proliferation and differentiation behaviors through cell–cell and cell–SNF interactions. The effects of SNFs on the proliferation as well as the osteogenic differentiation of MSCs were evaluated.

RESULTS

Morphology of a 3D SNF. To fabricate electrospun fabrics with an interconnected highly porous microstructure for cell ingrowth, a 3D SNF was prepared by the sol–gel

process.²⁴ Figure 1 shows the scanning electron microscopy (SEM) image of the SNF. The designed SNF has an average

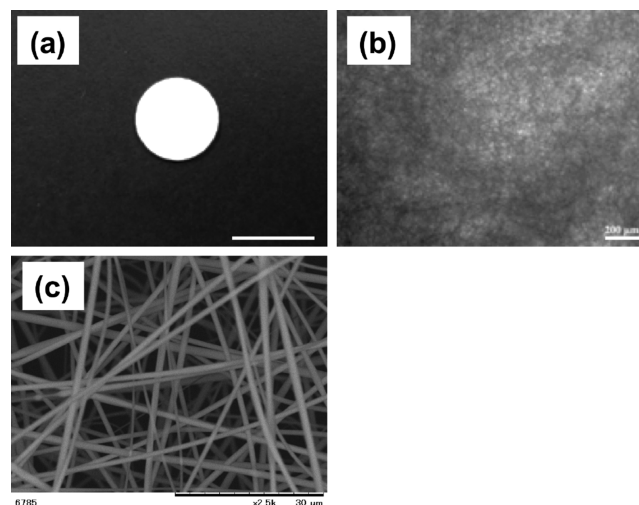


Figure 1. Morphologies of 3D SNFs. (a) Macroscopic image, (b) optical microscopic image, and (c) SEM image. Scale bars: 10 mm (a), 200 μm (b), and 30 μm (c).

pore size of 7.6 μm porosity and an average pore size of 7.6 μm ($n = 5$). The diameter of the fibers constituting the SNF was $704 \pm 280 \text{ nm}$ ($n = 50$). Many interconnected pores that may induce cellular migration and tissue ingrowth were provided by the random oriented nanofibers, preventing shrinkage during the cell culture because of the high mechanical strength of the SNF.

Mechanical Characteristics of SNFs. The mechanical properties of SNFs were characterized by the compression test and rheological analysis. In the compression test (Figure 2a,b), SNFs showed a compressive elastic modulus of over 1002 ± 85

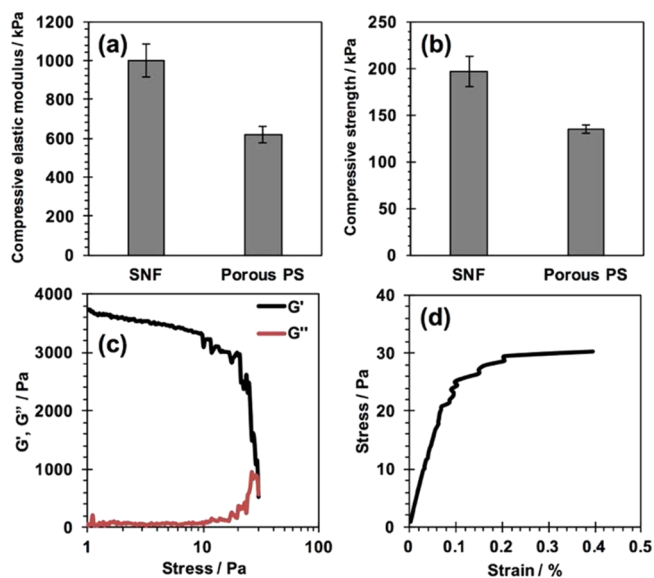


Figure 2. Mechanical properties of an SNF. (a,b) Compressive elastic modulus (a) and compressive strength (b) of the SNF and porous polystyrene substrate evaluated by the compression test. (c,d) Storage modulus G' and loss modulus G'' as a function of applied compression stress (c) and stress–strain curve obtained in strain sweep rheology experiments (d).

kPa and a compressive strength of 197 ± 17 , respectively. These values are higher than those of porous polystyrene disks used for the in vitro 3D cell culture. In the rheological analysis (Figure 2c,d), the fracture stress and fracture strain were 25.9 ± 8.3 Pa and $0.45 \pm 0.04\%$, respectively. Young's modulus was calculated as 3.27 ± 0.54 kPa.

Molecular Permeability of SNFs. The permeation behaviors of SNFs were investigated using fluorescein isothiocyanate (FITC)-dextran with a molecular weight of 20k. As shown in Figure 3, the time course of permeated

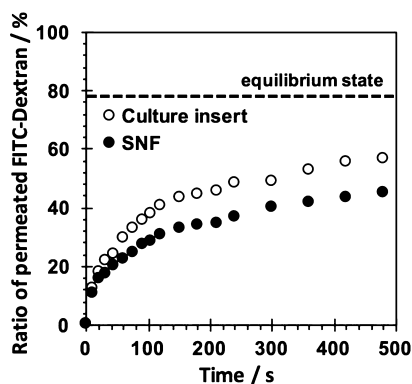


Figure 3. Permeation behaviors of the culture insert with and without the SNF using FITC-dextran (M_n : 20000) as the permeant. The amount of FITC-dextran at the equilibrium state estimated from the volume ratio of inside and outside of the culture insert was shown.

FITC-dextran through an SNF and a culture insert was estimated. The time-dependent permeation of FITC-dextran through an SNF was observed. The permeation of FITC through an SNF was rather slower than that of a culture insert without an SNF. Nevertheless, the obtained result suggested a sufficient permeability of SNFs for oxygen, minerals, nutrients, and secretions, which is important for maintaining the cell viability and vitality.

Adhesion and Proliferation of MSCs in the 3D SNF.

The adhesion and proliferation of MSCs on the 3D SNF were first examined using a water-soluble tetrazolium salt-8 (WST-8) assay and compared with those cultured on traditional 2D tissue culture-treated polystyrene (TCPS) plates. Figure 4a shows the number of cells adhered on the SNF and TCPS plates at 24 h after seeding. The number of cells adhered on the SNF was smaller than those on the TCPS plates, especially at a high seeding density. As can be seen in Figure 4b,c, the cell number of MSCs adhered on the TCPS plates grew linearly at a high seeding density (5 and 10×10^4 cells/well). In contrast to the cell growth on the TCPS plates, those seeded on the SNF at any density exponentially grew. The difference in cell growth was clearly demonstrated by the proliferation rate of MSCs, estimated on the SNF and TCPS plates from the calculated relative cell numbers to those at 24 h after seeding (Figure 4d,e). Although the MSCs seeded on the TCPS plates at a density of 1×10^4 cells/well detached from the TCPS surface from day 11 to day 14 because of overgrowth with a high proliferation rate (Figure 4e), the cells cultured in the 3D SNF were quite stable even after 14 days of culture (Figure 4d). These results suggested that the 3D SNF is suitable for the stable cell culture with a high proliferation rate, which is highly demanded in tissue engineering applications.

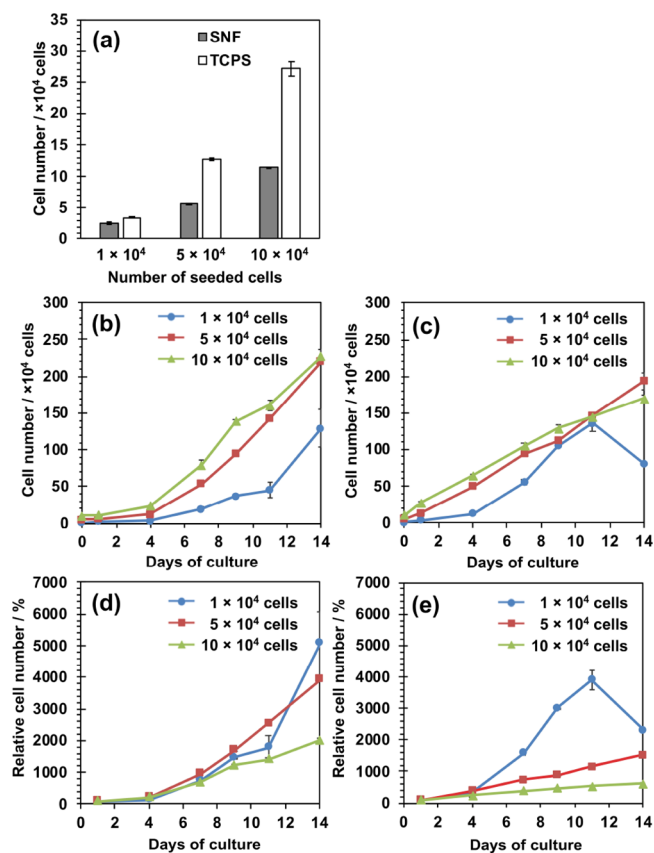


Figure 4. Adhesion and proliferation of human MSCs on 3D SNFs and TCPS plates measured using a WST-8 assay. (a) Number of cells on the 3D SNF and TCPS plates after 24 h of culture; (b,c) number of cells on the 3D SNF (b) and TCPS plates (c) seeded at various densities, 1 (circle), 5 (square), and 10 (triangle) $\times 10^4$ cells/well; (d,e) relative cell numbers to those after 24 h of culture on the 3D SNF (d) and TCPS plates (e) seeded at various densities, 1 (circle), 5 (square), and 10 (triangle) $\times 10^4$ cells/well. Data are shown as the mean \pm the standard error of the mean (S. E., $n = 2$).

Morphologies of MSCs Cultured in the 3D SNF. The morphologies of MSCs cultured in the 3D SNF were observed using confocal laser scanning microscopy (CLSM). The CLSM images of MSCs seeded at 1.5×10^5 cells/well after 7 and 14 days of culture are shown in Figure 5. Seven days after seeding, MSCs were detected at a depth of $36.96 \mu\text{m}$, but not at a depth of $66.87 \mu\text{m}$ (Figure 5b,c). Fourteen days after seeding, the number of cells at a depth of $36.96 \mu\text{m}$ was larger than that at 7 days (Figure 5e), and the cells were further detected even at a depth of $66.87 \mu\text{m}$ (Figure 5f). The results suggested that MSCs vertically migrated and proliferated in SNFs. The CLSM images of MSCs seeded at 3×10^4 and 3×10^5 cells/well after 7 and 14 days of culture are shown in Figures S1 and S2, respectively. Excepting that MSCs were seeded at 3×10^4 cells/well after 7 days of culture, the cells were highly stretched and migrated in SNFs. The thickness of cellular layers seeded at 3×10^4 , 1.5, and 3×10^5 cells/well were 8.3, 41, and $45 \mu\text{m}$ after 7 days and 50, 75, and $87 \mu\text{m}$ after 14 days, respectively.

Osteogenic Differentiation of MSCs in 3D SNFs. The osteogenic differentiation behaviors of MSCs in 3D SNFs were then investigated. After culture in an osteogenic differentiation medium up to 14 days, the alkaline phosphatase (ALP) activity was measured by a colorimetric method using *p*-nitrophenyl phosphate as a substrate. As shown in Figure 6, the ALP

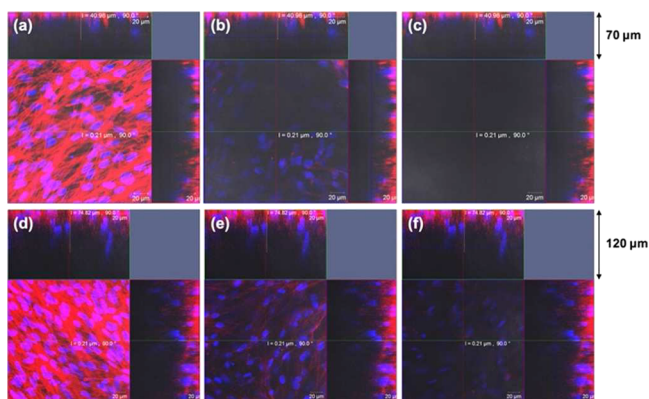


Figure 5. CLSM images showing the proliferation of MSCs on 3D SNFs 7 days (a–c) and 14 days (d–f) after seeding at a cell density of 1.5×10^5 . In each case, single optical slices near to the silica fabric surface [$1.76 \mu\text{m}$, (a,d)], middle [$36.96 \mu\text{m}$, (b,e)], and near the bottom [$66.87 \mu\text{m}$, (c,f)] are shown. Cellular nuclei and skeletons were stained with Hoechst 33342 (blue) and Alexa Fluor 594 phalloidin (red), respectively. Scale bars: $20 \mu\text{m}$.

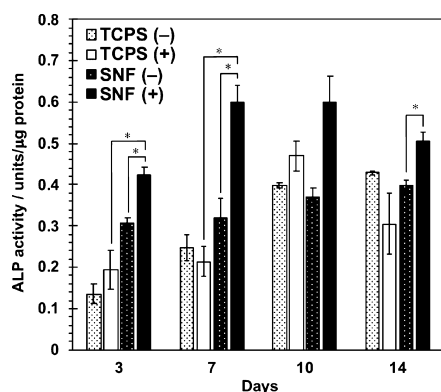


Figure 6. ALP activity of MSCs cultured on SNFs and TCPS plates under the normal medium (–) and the osteogenic differentiation medium (+). Data are shown as the mean \pm S. E. ($n = 4$). * indicates significance ($p < 0.05$, Student's t -test).

activity of cell cultures in SNFs was already higher than that on the TCPS plates after 3 days of culture. After 7 days of culture, the ALP activity in SNFs was much higher than that on the TCPS plates. The expression of an osteogenic differentiation marker gene, *RUNX2*, was investigated by real-time polymer chain reaction (PCR). Under both undifferentiating and differentiating conditions, the expression of *RUNX2* in cells cultured on SNFs was stronger than those on the TCPS plates (Figure 7a). In addition, the expression of *osteocalcin* (*OCN*) in cells cultured on SNFs tended to be higher than those on the TCPS plates at day 12 (Figure 7b). The osteogenic differentiation of MSCs was also evaluated by alizarin red staining. Although the influence of stratification of cells on microscopic observation cannot be excluded, after culture in an osteogenic differentiation medium for 14 days, the cells on SNFs stained more strongly and homogeneously than those on the TCPS plates (Figure 8b,d). The cells on SNFs were stained even in an undifferentiating condition (Figure 8a), suggesting the essential utility for a tissue-engineered construct, particularly bone formation. These results were certainly confirmed by the quantification of alizarin red staining.

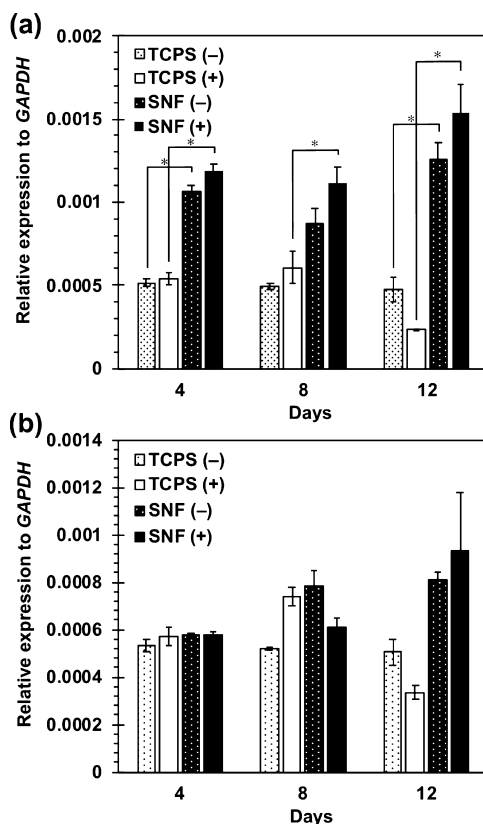


Figure 7. Expression of *RUNX2* (a) and *OCN* (b) in MSCs cultured on SNFs and TCPS plates under the normal medium (–) and the osteogenic differentiation medium (+). The signal intensity was normalized using that of a control housekeeping gene (human *GAPDH* gene). Data are shown as the mean \pm S. E. ($n = 2$). * indicates significance ($p < 0.05$, Student's t -test).

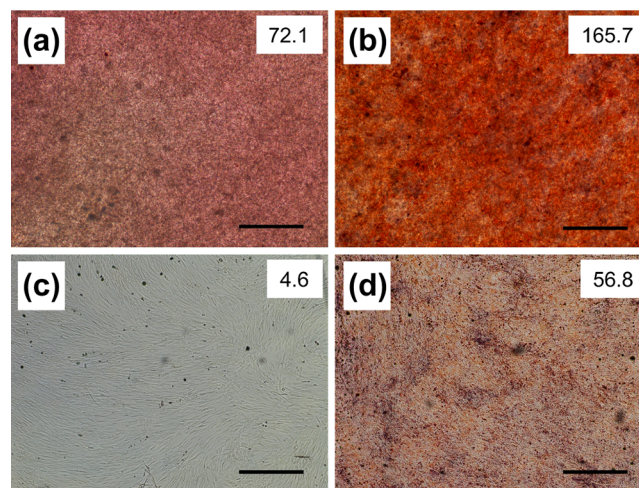


Figure 8. Alizarin red staining of MSCs on 3D SNFs (a,b) and TCPS plates (c,d) cultured in a Dulbecco's modified Eagle's medium (D-MEM(+)) (a,c) and an osteogenic differentiation medium (b,d) for 14 days. Scale bars: $500 \mu\text{m}$. The intensity of staining is shown in the upper right of each image.

DISCUSSION

In the present study, the proliferation and osteogenic differentiation of human bone marrow-derived MSCs in 3D SNFs were investigated. MSCs seeded on SNFs at any density

exponentially grew up to 14 days (Figure 4b), and the proliferation rate of cells in SNFs was much higher than that on the TCPS plates (Figure 4d,e). We have previously demonstrated that the fibroblast cultured in SNFs showed remarkable proliferation rates compared to the traditional 2D culture.²⁶ The results in this study suggested that MSCs vertically migrated and proliferated in SNFs without receiving signals of contact inhibition. In fact, the layer thickness of MSCs in SNFs after 14 days of culture was over 80 μm , which is much thicker than that of single layer of cells. This vertical migration of MSCs to form a 3D cell structure also supported proper cell growth with high proliferation rate and long-term stability.

After osteogenic differentiation, the ALP activity of cells on SNFs increased rapidly and remained high up to 14 days (Figure 6), and their *RUNX2* expression was much higher than those on the TCPS plates (Figure 7a). *RUNX2* is a transcription factor known as a master switch for the osteogenic differentiation of MSCs³⁵ and has been used as a marker gene for the early stage of osteogenic differentiation.³⁶ At day 12, the expression of OCN in cells cultured on SNFs tended to be higher than those on the TCPS plates at day 12 (Figure 7b). The osteocalcin protein coded by OCN is a secreted noncollagen matrix protein and a specific marker gene for the late stage of osteogenesis.³⁷ In some cases, there was no significant difference in the ALP activity and osteogenic differentiation markers whether or not bone differentiation was induced. It has been reported that osteogenic differentiation is induced even in the absence of the differentiation factor by the high-density culture³⁸ or in the culture on fibrous scaffolds;³⁹ therefore, it is possible that a significant difference was hard to be observed in the presence or absence of induction of bone differentiation. Evaluation of calcification of MSCs by alizarin red s staining after differentiation for 14 days (Figure 8) also indicated that SNFs enhanced their osteogenic differentiation.

The osteogenic differentiation of MSCs has been intensively investigated utilizing scaffolds such as HAp,⁴⁰ nonwoven nano- and microfibrillar scaffolds of polymers,^{17–21} or without scaffolds such as spheroid formation.⁴¹ Except for soluble factors, factors affecting the osteogenic differentiation of MSCs are classified into two categories. The first one is the interaction between cell–cell⁴² and cell–ECM.⁴³ The 3D nanofibrillar structures of SNFs share morphological similarities to collagen fibrils and enable to promote favorable biological responses for osteogenic differentiation. Furthermore, the high interconnectivity of SNFs allows the cells to interact with the surrounding cells. Another factor affecting the osteogenic differentiation of MSCs is the elasticity of substrates. The differentiation of MSCs was strongly affected by the elasticity of substrates and rigid matrices mimicking collagenous bone prove osteogenic differentiation.⁴⁴ Silica is a rigid substrate; therefore, it may also contribute to promote the osteogenic differentiation of MSCs.

A compressive strength of 0.2 MPa was obtained, which is almost tenth to the standard for a porous ceramic bone implant (2.4 MPa)⁴⁵ and slightly lower to the compressive strength of the trabecular bone, which has a compressive strength between 2 and 12 MPa.⁴⁶ However, it is well-known that the increase of mechanical properties of scaffolds has been obtained after tissue formation by in vitro differentiation or tissue growth after implantation. For example, it was reported that the strength and elastic modulus of the polymer hydrogel with MSCs were increased after osteogenic differentiation.⁴⁷

Furthermore, new bone formation was observed in hydroxyapatite ceramics throughout the pore network, and compressive strength was found to increase to ~ 30 MPa after 9 weeks of implantation because of tissue ingrowth. This increase in strength implies that it is not necessary to have a scaffold with a compressive strength equal to that of bone because the cell culture on the scaffold in vitro may create a biocomposite, leading to an increase in the strength.⁴⁸ Considering these increase effects in the mechanical property, SNFs seem to be potential materials for implantation. The characterization of the mechanical properties of SNF scaffolds with MSCs after osteogenic induction represents a forthcoming challenge.

It is also demonstrated that SNFs did not show a significant inhibitory effect on the permeability of the culture insert, which were widely used in research on cell–cell communication.⁴⁹ In fact, our previous study suggested that the paracrine factors secreted from the parenchymal primary hepatocyte placed in the bottom compartment of the trans-well system and the hepatic nonparenchymal cell fibroblast placed in the top insert were permeated each other through SNFs and enhanced functions of hepatocytes in a coculture system.²⁶ Therefore, the excellent permeability of SNFs seems to be effective for the osteogenesis of stem cells therein.

CONCLUSIONS

In this study, the proliferation and osteogenic differentiation of bone marrow-derived MSCs on 3D SNFs were investigated. MSCs migrated vertically inside the SNF, and their growth rate was much higher than those on the TCPS plates. In regenerative medicine, there is a strong demand for the expansion of cells collected from patients; therefore, a high growth rate of cells on SNFs meets the needs. Compared to conventional 2D culture on the TCPS plates, the osteogenic differentiation of MSCs was strongly promoted on SNFs as confirmed by the ALP activity, *RUNX2* expression, and the calcification of MSCs using alizarin red s staining. Furthermore, an excellent permeability of SNFs was confirmed by the transport of the dextran polymer with a molecular weight of 20k through SNFs. The higher permeability of SNFs for oxygen, minerals, nutrients, and cytokines, which are important for maintaining the cell viability and vitality, was indicated. These results suggested that SNFs are essential scaffolds not only for the in vitro cell assay system but also for the regeneration of bone defects using MSCs.

EXPERIMENTAL SECTION

Materials. Human serum fibronectin was purchased from Wako Pure Chemical Industries, Ltd. (Osaka, Japan). All chemicals were purchased from Wako Pure Chemicals, Inc., and used without further purification. The 24-well TCPS plates were obtained from Becton, Dickinson and Co. (Franklin Lakes, NJ).

Cell Culture. Human bone marrow-derived MSCs with an extended life span through retroviral transduction UE7T-13 cells⁵⁰ were obtained from Japanese Collection of Research Bioresources (JCRB) Cell Bank, National Institute of Biomedical Innovation. The UE7T-13 cells were maintained in a standard D-MEM (Life Technologies Corp., Carlsbad, CA) supplemented with 10% (v/v) fetal bovine serum (SAFC Biosciences, Inc., Carlsbad, CA), 100 U/mL of penicillin, and 100 $\mu\text{g}/\text{mL}$ of streptomycin (Sigma-Aldrich Co. LLC, St.

Louis, MO) (D-MEM(+)) at 37 °C under a humidified 5% CO₂ atmosphere.

Preparation of Silica Fiber Nonwoven Fabrics.

Tetraethoxysilane as a metal compound, ethanol as a solvent, water for hydrolysis, and 1 N hydrochloric acid as a catalyst were mixed at a molar ratio of 1:5:2:0.003, refluxed at a temperature of 78 °C for 10 h, followed by removing a solvent to concentrate, further followed by heating, thereby a sol solution was formed. Using the resulted sol solution as a spinning solution, according to a plate-spinning method that is an electrospinning method, the gel silica fiber webs were prepared. These SNF cell scaffolds are already commercially available as Cellbed from Japan Vilene Co. Ltd. The morphologies of SNFs used in this study were observed using a scanning electron microscope (Miniscope TM3030, Hitachi Ltd., Tokyo, Japan) with an acceleration voltage of 15 kV.

Mechanical Characteristic Analysis. The mechanical properties of SNFs were characterized by the compression test and rheological analysis using SNFs with a diameter of 10 mm and a thickness of 182 μm. All measurements were performed at 20 °C. In the compression test, the compressive elastic modulus and compressive strength of SNFs were tested using a universal tester (Autograph AGS-J; Shimadzu Corp., Kyoto, Japan) with a 500 N load cell. The samples were axially compressed at a rate of 0.5 mm/min, and the stress–strain curves were collected and analyzed using TRPEZIUM X software. The compressive elastic modulus and compressive strength were determined from the slope of the stress–strain curves and yield stress, respectively. As a control, porous polystyrene disks (Alvetex Scaffold 12-well insert, ReproCELL Inc., Yokohama, Japan) with a diameter of 16 mm, a pore size of 36–40 μm, a porosity of >90%, and a thickness of 200 μm were used. Each experiment was performed in duplicate and shown as the mean ± S. E. In the rheological analysis, strain sweep rheology experiments were performed on a HAAKE MARS rotational rheometer (Thermo Scientific, Inc., Waltham, MA). The SNF was placed on the bottom stage. Then, a top plate was approached until the load was monitored to 0.1 N, and the SNF was compressed by the upper plate at a strain rate of 1 mm/min. Young's modulus was calculated as the initial slope of the stress–strain curve in the range of strain from 0 to 10%. Each experiment was performed in triplicate and shown as the mean ± S. E.

Permeability Assay. The molecular permeability of SNFs was investigated using FITC-dextran (M_n : 20 000, Sigma-Aldrich, Co., LLC). Briefly, after the construction of a transwell system (12-well plates) filled with 2.9 mL of D-MEM, the SNF was placed in the top insert. When 100 μL of 1.5 mM FITC-dextran in the D-MEM was added to the top insert, the experiment was started. The sample (100 μL) was collected from the medium in the lower chamber to evaluate the concentration of permeated FITC-dextran at each time point. A similar volume of fresh culture medium was added to the lower chamber after the sample was collected each time to maintain the volume. The concentration of permeated FITC-dextran was determined by the measurement of fluorescence intensity (λ_{ex} = 494 nm, λ_{em} = 518 nm) using a microplate reader. Permeability was evaluated in % as compared to the total amount of FITC-dextran added.

Adhesion and Proliferation of MSCs on SNFs. Each well of 96-well plates with the SNF was pretreated with 70% (v/v) ethanol and phosphate-buffered saline (PBS) three times

in order to prevent bubbles inside the fabrics. Cells (1, 5, and 10×10^4) dispersed in 100 μL of D-MEM(+) were seeded on each well of 96-well plates with SNFs and TCPS plates and cultured at 37 °C. Media were changed every 3 days, and the cells were cultured for 14 days. The cell numbers were measured using a WST-8 assay. A WST-8 premix solution (20 μL of WST-8 working solution (Cell Counting Kit-8, Dojindo Laboratories, Co. Ltd., Kumamoto, Japan) and 180 μL of D-MEM(+)) was added to each well and incubated at 37 °C for 30 min. Absorbance at 450 nm was measured using a microplate reader (Varioskan Flash, Thermo Fisher Scientific, Inc.). The number of cells was determined using the absorbance value of a calibration curve for the known number of cells. Each experiment was performed in duplicate and shown as the mean ± S. E.

CLSM Observation of MSCs on SNFs. Cells (3×10^4 , 1.5 , and 3×10^5) dispersed in 500 μL D-MEM(+) were seeded on SNFs set in a 12-well culture insert (Becton, Dickinson and Co.) and cultured at 37 °C. Media were changed every 3 days, and the cells were cultured for 7 and 14 days. The cells were treated with 5 μg/mL Hoechst 33342 (Dojindo laboratories) in D-MEM(+) for an hour under dark condition. Then, the cells were washed three times with PBS and fixed with 4 wt % paraformaldehyde solutions in PBS for 20 min, followed by permeation with 0.5% TritonX-100 solution for 2 min. The cells were treated with 1% Alexa Fluor 594 phalloidin (Life Technologies, Corp.) for 2 h. After washing three times with PBS, the cells were observed by a confocal laser scanning microscope (LSM-710, Carl Zeiss AG, Oberkochen, Germany).

Osteogenic Differentiation of MSCs on SNFs. MSCs (3×10^5) dispersed in 500 μL of D-MEM(+) were seeded on SNFs set in a 12-well culture insert and precultured for 7 days. MSCs (3×10^4) were seeded on fibronectin-coated 24-well TCPS plates and precultured until the cells reached confluency (about 3 days). Then, the cell culture medium was changed to the osteogenic differentiation medium (PromoCell, GmbH, Heidelberg, Germany). Media were changed every 3 days, and the cells were cultured for further 14 days. The cells were solubilized in lysis buffer (50 mM Tris-HCl, pH 8.0, 150 mM NaCl, 1% NP-40) for 30 min on ice, and the total protein concentration was determined using a Pierce BCA Protein Assay Kit (Thermo Fisher Scientific, Inc.) according to the manufacturer's instructions.

ALP Assay. The ALP activity of the lysate of MSCs with and without osteogenic induction was measured using a Lab Assay ALP kit (Wako pure chemicals, Inc.) according to the manufacturer's instructions. Cell lysate (20 μL) was added to 6.7 mM of *p*-nitrophenyl phosphate in 100 mM carbonate buffer (pH 9.8) containing 2 mM MgCl₂ and incubated at 37 °C for 15 min. After the addition of stop solution (200 mM HCl), the absorbance at 405 nm was measured using a microplate reader and normalized to the total amount of proteins in each sample lysate. Each experiment was performed in quadruplicate and shown as the mean ± S. E.

Real-Time Reverse Transcription-PCR. Total RNA was extracted from cultured cells with an RNeasy mini kit (Qiagen, Inc., Hilden, Germany) combined with Trizol (Thermo Fisher Scientific Inc., Waltham, MA). Briefly, the cells were dispersed and homogenized in Trizol using Powermasher (Nippi, Inc., Tokyo, Japan) and biomasher II (Nippi, Inc.), and total RNA was extracted according to the manufacturer's instructions. cDNA was generated with a ReverTra Ace qPCR RT Master

Mix with a gDNA Remover (Toyobo Co., Ltd., Osaka, Japan) according to the manufacturer's instructions. Real-time reverse transcriptase (RT)-PCR was performed using the Thunderbird SYBR qPCR Mix (Toyobo Co., Ltd.) on an ABI PRISM 7900HT sequence detection system (Applied Biosystems, Inc., Foster City, CA). The relative quantification was calculated via the $\Delta\Delta C_t$ method and normalized against the housekeeping *GAPDH*. The following primers were used: *RUNX2*,⁵¹ 5'-cactggcgtgcaacaaga-3' (sense) and 5'-catgacagtaaccacagtcctc-3' (antisense); *OCN*,³⁸ 5'-ccacatcggcttcaggag-3' (sense) and 5'-gcaaggggaagaggaaaga-3' (antisense); and *GAPDH*, 5'-agcaagagcacaagaggaaga-3' (sense) and 5'-gaggggagattcagtggtg-3' (antisense).

Alizarin Red Staining. Alizarin red s (2 g; Sigma-Aldrich, Co., LLC.) was dissolved in 100 mL of ultrapure water, and the pH of the solution was adjusted to 6.0 with NH_4OH . The solution was filtered through 0.22 μm of the poly(vinylidene difluoride) membrane (Merck KGaA, Darmstadt, Germany). MSCs cultured on SNFs and TCPS plates in D-MEM(+) and osteogenic differentiation medium for 14 days were fixed with 4% formalin in PBS containing 10% glycerol for an hour. Then, the cells were stained with an alizarin solution at room temperature for 5 min and washed two times with PBS. The samples were observed using microscopy (ECLIPSE LV100, Nikon Corp., Tokyo, Japan). The intensity of alizarin red staining was quantified using ImageJ as follows. The individual red, green, and blue channels were extracted, and the blue channel was subtracted from the red channel. Then, the intensity of the resultant red channel was quantified.

■ ASSOCIATED CONTENT

📄 Supporting Information

The Supporting Information is available free of charge on the ACS Publications website at DOI: 10.1021/acsomega.8b01139.

CLSM images showing the proliferation of MSCs on 3D SNFs after seeding at cell densities of 3×10^4 and 3×10^5 (PDF)

■ AUTHOR INFORMATION

Corresponding Author

*E-mail: h.otsuka@rs.kagu.tus.ac.jp. Phone: +81-3-5228-8265. Fax: +81-3-5261-4631 (H.O.).

ORCID

Kazutoshi Iijima: 0000-0001-9173-1666

Mineo Hashizume: 0000-0001-8162-5173

Hidenori Otsuka: 0000-0003-0183-8510

Present Address

¹Faculty of Engineering, Yokohama National University, 79-5 Tokiwadai, Hodogaya-ku, Yokohama 240-8501, Japan.

Author Contributions

The manuscript was written through contributions from all authors. All authors have given approval to the final version of the manuscript.

Notes

The authors declare no competing financial interest.

■ ABBREVIATIONS

ECM, extracellular matrix; SNF, silica nonwoven fabric; MSC, mesenchymal stem cell; TCPS, tissue culture-treated polystyrene; D-MEM, Dulbecco's modified Eagle's medium; SEM,

scanning electron microscopy; WST-8, water-soluble tetrazolium salt-8; CLSM, confocal laser scanning microscopy; RT-PCR, reverse transcription-polymer chain reaction; FITC, fluorescein isothiocyanate; S. E., standard error of the mean

■ REFERENCES

- (1) Pampaloni, F.; Reynaud, E. G.; Stelzer, E. H. K. The Third Dimension Bridges the Gap Between Cell Culture and Live Tissue. *Nat. Rev. Mol. Cell Biol.* **2007**, *8*, 839–845.
- (2) Fennema, E.; Rivron, N.; Rouwkema, J.; van Blitterswijk, C.; de Boer, J. Spheroid Culture as a Tool for Creating 3D Complex Tissues. *Trends Biotechnol.* **2013**, *31*, 108–115.
- (3) Otsuka, H.; Hirano, A.; Nagasaki, Y.; Okano, T.; Horiike, Y.; Kataoka, K. Two-Dimensional Multiaarray Formation of Hepatocyte Spheroids on a Microfabricated PEG-Brush Surface. *ChemBioChem* **2004**, *5*, 850–855.
- (4) Koutsopoulos, S. Self-assembling Peptide Nanofiber Hydrogels in Tissue Engineering and Regenerative Medicine: Progress, Design Guidelines, and Applications. *J. Biomed. Mater. Res. A* **2016**, *104*, 1002–1016.
- (5) Hollister, S. J. Porous Scaffold Design for Tissue Engineering. *Nat. Mater.* **2005**, *4*, 518–524.
- (6) Hong, J. K.; Madihally, S. V. Next Generation of Electrospun Fibers for Tissue Regeneration. *Tissue Eng., Part B* **2011**, *17*, 125–142.
- (7) Richardson, S. M.; Kalamegam, G.; Pushparaj, P. N.; Matta, C.; Memic, A.; Khademhosseini, A.; Mobasher, R.; Poletti, F. L.; Hoyland, J. A.; Mobasher, A. Mesenchymal Stem Cells in Regenerative Medicine: Focus on Articular Cartilage and Intervertebral Disc Regeneration. *Methods* **2016**, *99*, 69–80.
- (8) Pittenger, M. F.; Mackay, A. M.; Beck, S. C.; Jaiswal, R. K.; Douglas, R.; Mosca, J. D.; Moorman, M. A.; Simonetti, D. W.; Craig, S.; Marshak, D. R. Multilineage Potential of Adult Human Mesenchymal Stem Cells. *Science* **1999**, *284*, 143–147.
- (9) De Francesco, F.; Ricci, G.; D'Andrea, F.; Nicoletti, G. F.; Ferraro, G. A. Human Adipose Stem Cells: From Bench to Bedside. *Tissue Eng., Part B* **2015**, *21*, 572–584.
- (10) Jaiswal, N.; Haynesworth, S. E.; Caplan, A. I.; Bruder, S. P. Osteogenic Differentiation of Purified, Culture-Expanded Human Mesenchymal Stem Cells In Vitro. *J. Cell. Biochem.* **1997**, *64*, 295–312.
- (11) Mackay, A. M.; Beck, S. C.; Murphy, J. M.; Barry, F. P.; Chichester, C. O.; Pittenger, M. F. Chondrogenic Differentiation of Cultured Human Mesenchymal Stem Cells from Marrow. *Tissue Eng.* **1998**, *4*, 415–428.
- (12) Nuttall, M. E.; Patton, A. J.; Olivera, D. L.; Nadeau, D. P.; Gowen, M. Human Trabecular Bone Cells Are Able to Express Both Osteoblastic and Adipocytic Phenotype: Implications for Osteopenic Disorders. *J. Bone Miner. Res.* **1998**, *13*, 371–382.
- (13) Wakitani, S.; Saito, T.; Caplan, A. I. Myogenic Cells Derived from Rat Bone Marrow Mesenchymal Stem Cells Exposed to 5-Azacytidine. *Muscle Nerve* **1995**, *18*, 1417–1426.
- (14) Makino, S.; Fukuda, K.; Miyoshi, S.; Konishi, F.; Kodama, H.; Pan, J.; Sano, M.; Takahashi, T.; Hori, S.; Abe, H.; Hata, J.-i.; Umezawa, A.; Ogawa, S. Cardiomyocytes Can Be Generated from Marrow Stromal Cells In Vitro. *J. Clin. Invest.* **1999**, *103*, 697–705.
- (15) Kon, E.; Filardo, G.; Roffi, A.; Di Martino, A.; Hamdan, M.; De Pasqual, L.; Merli, M. L.; Marzocchi, M. Bone Regeneration with Mesenchymal Stem Cells. *Clin. Cases Miner. Bone Metab.* **2012**, *9*, 24–27.
- (16) Moradi, S. L.; Golchin, A.; Hajishafieha, Z.; Khani, M.-M.; Ardeshirylajimi, A. Bone Tissue Engineering: Adult Stem Cells in Combination with Electrospun Nanofibrous Scaffolds. *J. Cell. Physiol.* **2018**, *233*, 6509–6522.
- (17) Li, W.-J.; Tuli, R.; Huang, X.; Laquerriere, P.; Tuan, R. S. Multilineage Differentiation of Human Mesenchymal Stem Cells in a Three-dimensional Nanofibrous Scaffold. *Biomaterials* **2005**, *26*, 5158–5166.

- (18) Cao, Y.; Li, D.; Shang, C.; Yang, S. T.; Wang, J.; Wang, X. Three-Dimensional Culture of Human Mesenchymal Stem Cells in a Polyethylene Terephthalate Matrix. *Biomed. Mater.* **2010**, *5*, 065013.
- (19) Ardeshiryajimi, A.; Mossahebi-Mohammadi, M.; Vakilian, S.; Langroudi, L.; Seyedjafari, E.; Atashi, A.; Soleimani, M. Comparison of Osteogenic Differentiation Potential of Human Adult Stem Cells Loaded on Bioceramic-Coated Electrospun Poly (L-lactide) Nanofibers. *Cell Prolif.* **2015**, *48*, 47–58.
- (20) Pournaqi, F.; Ghiasee, A.; Vakilian, S.; Ardeshiryajimi, A. Improved Proliferation and Osteogenic Differentiation of Mesenchymal Stem Cells on Polyaniline Compositing by Polyethersulfone Nanofibers. *Biologicals* **2017**, *45*, 78–84.
- (21) Ardeshiryajimi, A.; Farhadian, S.; Jamshidi Adegani, F.; Mirzaei, S.; Soufi Zomorrod, M.; Langroudi, L.; Doostmohammadi, A.; Seyedjafari, E.; Soleimani, M. Enhanced osteoconductivity of polyethersulphone nanofibres loaded with bioactive glass nanoparticles in in vitro and in vivo models. *Cell Prolif.* **2015**, *48*, 455–464.
- (22) Yamaguchi, T.; Sakai, S.; Kawakami, K. Application of Silicate Electrospun Nanofibers for Cell Culture. *J. Sol-Gel Sci. Technol.* **2008**, *48*, 350–355.
- (23) Yamaguchi, T.; Sakai, S.; Watanabe, R.; Tarao, T.; Kawakami, K. Heat Treatment of Electrospun Silicate Fiber Substrates Enhances Cellular Adhesion and Proliferation. *J. Biosci. Bioengin.* **2010**, *109*, 304–306.
- (24) Watanabe, R.; Tarao, T.; Kawabe, M.; Yamaguchi, T.; Kawakami, K. U.S. Patent 2,011,027,492,7 A1, 2011.
- (25) Yamaguchi, Y.; Deng, D.; Sato, Y.; Hou, Y. T.; Watanabe, R.; Sasaki, K.; Kawabe, M.; Hirano, E.; Morinaga, T. Silicate Fiber-Based 3D Cell Culture System for Anticancer Drug Screening. *Anticancer Res.* **2013**, *33*, 5301–5309.
- (26) Otsuka, H.; Sasaki, K.; Okimura, S.; Nagamura, M.; Watanabe, R.; Kawabe, M. Contribution of Fibroblasts Cultured on 3D Silica Nonwoven Fabrics to Cocultured Hepatocytes Function. *Chem. Lett.* **2014**, *43*, 343–345.
- (27) Ahola, M. S.; Säilynoja, E. S.; Raitavuo, M. H.; Vaahtio, M. M.; Salonen, J. I.; Yli-Urpo, A. U. O. In vitro release of heparin from silica xerogels. *Biomaterials* **2001**, *22*, 2163–2170.
- (28) Sepulveda, P.; Jones, J. R.; Hench, L. L. In Vitro Dissolution of Melt-Derived 45S5 and Sol-Gel Derived 58S Bioactive Glasses. *J. Biomed. Mater. Res. A* **2002**, *61*, 301–311.
- (29) Jones, J. R.; Ehrenfried, L. M.; Hench, L. L. Optimising Bioactive Glass Scaffolds for Bone Tissue Engineering. *Biomaterials* **2006**, *27*, 964–973.
- (30) van Gestel, N. A.; Geurts, J.; Hulsen, D. J.; van Rietbergen, B.; Hofmann, S.; Arts, J. J. Clinical Applications of S53P4 Bioactive Glass in Bone Healing and Osteomyelitic Treatment: A Literature Review. *Biomed. Res. Int.* **2015**, *2015*, 684826.
- (31) Arcos, D.; Vallet-Regí, M. Sol-Gel Silica-Based Biomaterials and Bone Tissue Regeneration. *Acta Biomater.* **2010**, *6*, 2874–2888.
- (32) Pereira, M. M.; Clark, A. E.; Hench, L. L. Effect of Texture on the Rate of Hydroxyapatite Formation on Gel-Silica Surface. *J. Am. Ceram. Soc.* **1995**, *78*, 2463–2468.
- (33) Okii, N.; Nishimura, S.; Kurisu, K.; Takeshima, Y.; Uozumi, T. In Vivo Histological Changes Occurring in Hydroxyapatite Cranial Reconstruction. Case Report. *Neurol. Med. Chir.* **2001**, *41*, 100–104.
- (34) Hench, L. L.; Polak, J. M. Third-Generation Biomedical Materials. *Science* **2002**, *295*, 1014–1017.
- (35) Augello, A.; De Bari, C. The Regulation of Differentiation in Mesenchymal Stem Cells. *Hum. Gene Ther.* **2010**, *21*, 1226–1238.
- (36) Westrin, M.; Xie, M.; Olderøy, M. Ø.; Sikorski, P.; Strand, B. L.; Standal, T. Osteogenic Differentiation of Human Mesenchymal Stem Cells in Mineralized Alginate Matrices. *PLoS One* **2015**, *10*, No. e0120374.
- (37) Takagaki, Y. M.; Kakai, Y.; Satoyoshi, M.; Kawano, E.; Suzuki, Y.; Kawase, T.; Saito, S. Matrix Mineralization and the Differentiation of Osteocyte-Like Cells in Culture. *J. Bone Miner. Res.* **1995**, *10*, 231–242.
- (38) Thibault, R. A.; Scott Baggett, L.; Mikos, A. G.; Kasper, F. K. Osteogenic Differentiation of Mesenchymal Stem Cells on Pregelatinated Extracellular Matrix Scaffolds in the Absence of Osteogenic Cell Culture Supplements. *Tissue Eng., Part A* **2010**, *16*, 431–440.
- (39) Vo, T. N.; Tabata, Y.; Mikos, A. G. Effects of cellular parameters on the in vitro osteogenic potential of dual-gelling mesenchymal stem cell-laden hydrogels. *J. Biomater. Sci., Polym. Ed.* **2016**, *27*, 1277–1290.
- (40) Iijima, K.; Suzuki, R.; Iizuka, A.; Ueno-Yokohata, H.; Kiyokawa, N.; Hashizume, M. Surface Functionalization of Tissue Culture Polystyrene Plates with Hydroxyapatite Under Body Fluid Conditions and Its Effect on Differentiation Behaviors of Mesenchymal Stem Cells. *Colloids Surf., B* **2016**, *147*, 351–359.
- (41) Miyagawa, Y.; Okita, H.; Hiroyama, M.; Sakamoto, R.; Kobayashi, M.; Nakajima, H.; Katagiri, Y. U.; Fujimoto, J.; Hata, J.-I.; Umezawa, A.; Kiyokawa, N. A Microfabricated Scaffold Induces the Spheroid Formation of Human Bone Marrow-Derived Mesenchymal Progenitor Cells and Promotes Efficient Adipogenic Differentiation. *Tissue Eng., Part A* **2011**, *17*, 513–521.
- (42) Wang, X.; Song, W.; Kawazoe, N.; Chen, G. The Osteogenic Differentiation of Mesenchymal Stem Cells by Controlled Cell-Cell Interaction on Micropatterned Surfaces. *J. Biomed. Mater. Res. A* **2013**, *101*, 3388–3395.
- (43) Frith, J. E.; Mills, R. J.; Hudson, J. E.; Cooper-White, J. J. Tailored Integrin-Extracellular Matrix Interactions to Direct Human Mesenchymal Stem Cell Differentiation. *Stem Cells Dev.* **2012**, *21*, 2442–2456.
- (44) Engler, A. J.; Sen, S.; Sweeney, H. L.; Discher, D. E. Matrix Elasticity Directs Stem Cell Lineage Specification. *Cell* **2006**, *126*, 677–689.
- (45) *Implants for Surgery—Hydroxyapatite—Part 1: Ceramic Hydroxyapatite*. BS ISO 13779-1, 2000.
- (46) Carter, D.; Hayes, W. Bone Compressive Strength: The Influence of Density and Strain Rate. *Science* **1976**, *194*, 1174–1176.
- (47) Liao, H.-T.; Chen, C.-T.; Chen, J.-P. Osteogenic Differentiation and Ectopic Bone Formation of Canine Bone Marrow-Derived Mesenchymal Stem Cells in Injectable Thermo-Responsive Polymer Hydrogel. *Tissue Eng., Part C* **2011**, *17*, 1139–1149.
- (48) Tamai, N.; Myoui, A.; Tomita, T.; Nakase, T.; Tanaka, J.; Ochi, T.; Yoshikawa, H. Novel hydroxyapatite ceramics with an interconnective porous structure exhibit superior osteoconduction in vivo. *J. Biomed. Mater. Res.* **2002**, *59*, 110–117.
- (49) Holt, D. J.; Chamberlain, L. M.; Grainger, D. W. Cell-Cell Signaling in Co-Cultures of Macrophages and Fibroblasts. *Biomaterials* **2010**, *31*, 9382–9394.
- (50) Mori, T.; Kiyono, T.; Imabayashi, H.; Takeda, Y.; Tsuchiya, K.; Miyoshi, S.; Makino, H.; Matsumoto, K.; Saito, H.; Ogawa, S.; Sakamoto, M.; Hata, J.-I.; Umezawa, A. Combination of hTERT and bmi-1, E6, or E7 Induces Prolongation of the Life Span of Bone Marrow Stromal Cells from an Elderly Donor without Affecting Their Neurogenic Potential. *Mol. Cell Biol.* **2005**, *25*, 5183–5195.
- (51) Gao, Y.; Zhao, G.; Li, D.; Chen, X.; Pang, J.; Ke, J. Isolation and Multiple Differentiation Potential Assessment of Human Gingival Mesenchymal Stem Cells. *Int. J. Mol. Sci.* **2014**, *15*, 20982–20996.